JACS
JOURNAL OF THE AMERICAN CHEMICAL SOCIETY
Article
pubs.acs.org/JACS

A Two-Dimensional Polymer from the Anthracene Dimer and Triptycene Motifs

Radha Bhola,[†] Payam Payamyar,[‡] Daniel J. Murray,[†] Bharat Kumar,[†] Aaron J. Teator,[†] Martin U. Schmidt,[§] Sonja M. Hammer,[§] Animesh Saha,[‡] Junji Sakamoto,[‡] A. Dieter Schlüter,[‡] and Benjamin T. King*[,†]

[†]Department of Chemistry, University of Nevada, Reno, Nevada 89557-0216, United States

[‡]Department of Materials, Laboratory of Polymer Chemistry, Institute of Polymers, ETH Zürich, Wolfgang-Pauli-Strasse 10, CH-8093 Zürich, Switzerland

[§]Institute of Inorganic and Analytical Chemistry, Goethe University, Max-von-Laue-Strasse 7, 60438 Frankfurt am Main, Germany

Supporting Information

ABSTRACT: A two-dimensional polymer (2DP) based on the dimerization of anthraceno groups arranged in a triptycene motif is reported. A photoinduced polymerization is performed in the crystalline state and gives a lamellar 2DP via a crystal-to-crystal (but not single-crystal to single-crystal) transformation. Solvent-induced exfoliation provides monolayer sheets of the 2DP. The 2DP is considered to be a tiling, a mathematical approach that facilitates structural elucidation.

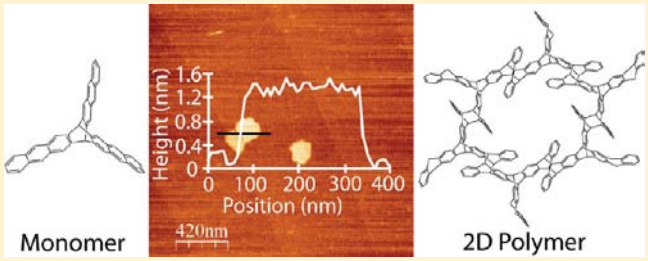

INTRODUCTION

We report the synthesis of a two-dimensional polymer (2DP) based on triptycene cores linked by anthracene dimers. We begin by defining 2DPs. While two-dimensional polymers (2DPs) can be thought of as a monolayer of repeat units (RUs) connected by robust bonds to give sheets, topology provides a more precise definition. A 2DP can be represented as a *tiling*, where the RUs are vertices, the connection between the RUs are edges, and the edges outline tiles that can cover the plane without gaps or overlaps. O'Keeffe and Hyde have considered the packing of layered crystals using similar ideas.[1] Consider graphene in terms of this topological definition. Carbon atoms are the RUs, the C−C bonds are the edges, and these edges form hexagonal tiles that cover the plane. This topological definition is simpler than and mostly consistent with earlier definitions,[2] but it embodies the sheet-like character of 2DPs and distinguishes 2DPs from other thin, cross-linked polymers. While periodicity facilitates characterization and will be useful in many applications, it is not an essential feature of 2DPs and is not required by this topological definition. This definition also lets us analyze the structure of 2DPs in a useful mathematical framework.

Graphene is the 2DP prototype.[3] While the properties of graphene are remarkable, its structure is essentially fixed. The rational synthesis of 2DPs[2] can provide 2DPs with tailored structures and function that complement those of graphene. This is our motivation.

Two main approaches to the preparation of 2DPs can be identified. The first approach involves a synthesis of a 2DP from monomers confined to a surface. The second approach involves the physical exfoliation of a crystal comprising layers. The layered crystal can be a naturally occurring, like graphite, or synthetic. The physical exfoliation of a synthetic layered crystal was recently shown[4] to be viable and is the approach we follow here.

The surface confinement approach to 2DPs can be performed on solid faces, notably on atomically flat faces of single metal crystals, allowing the polymerization reactions to be followed by scanning tunneling microscopy.[5−7] This approach provides outstanding analytical capability but provides only small sheets, usually less than a few hundred nm^2, in small quantities. Thin, multilayer covalent organic frameworks (COFs) have also been grown on single-sheet graphene substrates.[8] Polymerization on liquid surfaces, as was pioneered by Gee[9] in 1935 and advanced by Kunitake[10] and Michl,[11] is another useful surface confinement approach. Bauer, Schlüter, and Sakamoto[12,13] also have prepared monolayer sheets that may qualify as 2DPs by confinement at liquid surfaces. An advantage of the liquid surface approach is its ability to provide large (cm^2 or more) sheets.

In the second approach, layered crystals, which can be natural or synthetic, are exfoliated. Various layered inorganic materials, most notably graphite, have been exfoliated into monolayers.[14−17] The layered covalent organic frameworks[18,19] (COFs) and metal organic frameworks[20,21] (MOFs) are also beginning to receive attention. Kissel, Schlüter, and Sakamoto recently reported the solid-state photopolymerization of a

Received: May 6, 2013
Published: September 17, 2013

   dx.doi.org/10.1021/ja404351p | J. Am. Chem. Soc. 2013, 135, 14134−14141

sophisticated triple-anthracene monomer to give a 2DP and its exfoliation to single sheets.[4]

We have prepared a 2DP by solid-state polymerization of the antrip monomer (Figure 1), which has three anthraceno blades

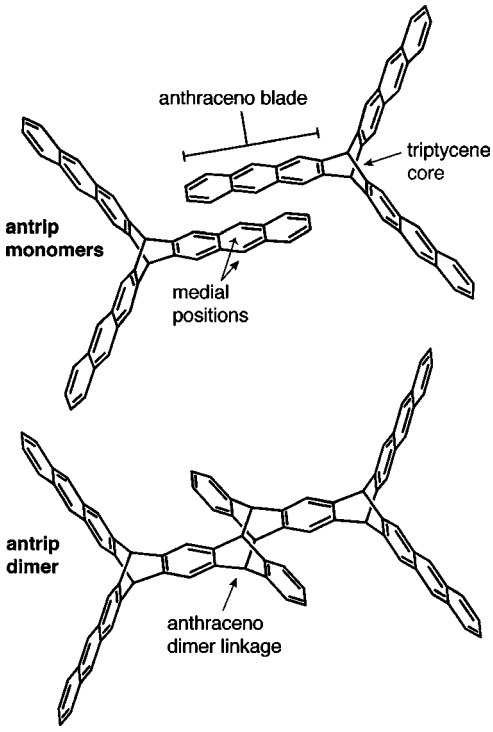

Figure 1. Structure of the antrip monomer and dimer.

in a triptycene motif. Our approach is related to the exfoliation of a layered COF or MOF but has some important differences. A COF or MOF is usually prepared in a simultaneous reaction and crystallization process: bonds are made while the crystal forms. In our approach, we have separated crystallization and bond formation by relying on an initial crystallization to organize the monomers and subsequent solid-state photopolymerization[22,23] to give the 2DP.

RESULTS

Optimization of the synthesis of antrip, which was first reported by Swager in 2001,[24] (Scheme S1 in the Supporting Information (SI)), provided sufficient quantities (0.1 g) for crystallization, polymerization, and exfoliation studies. The dimer of a triptycene bearing a single anthraceno blade was prepared in 1987.[25]

Crystals grown from a variety of solvents were screened for photopolymerization by monitoring changes in solubility and IR spectra after UV irradiation. While several solvates photopolymerized, we focused on the $P2_1/c$ polymorph of the benzene solvate because the crystals grown from this solvent were larger and their photopolymerization was clean.

In the $P2_1/c$ polymorph of the benzene solvate, the antrip molecules form two sets of rows, tilted by 35.3°, and these rows align to form hexagonal channels that are filled by solvent. The rows are formed by the cofacial arrangement of two of the three anthraceno blades (Figure 2). The chloroform, THF, and fluorobenzene solvates pack in the same way with the two sets of rows also tilted by 35° ± 3°.[26]

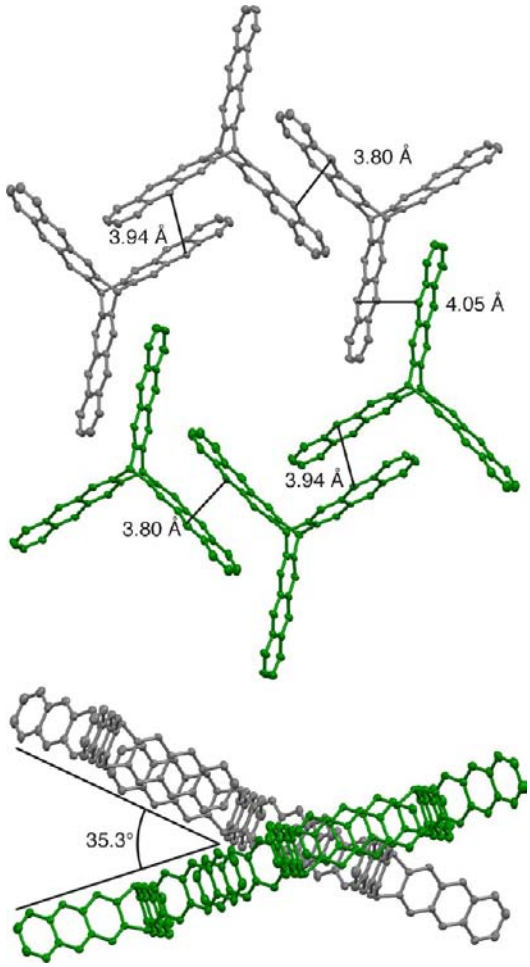

Figure 2. Packing of the $P2_1/c$ polymorph of the benzene solvate, looking down the hexagonal channels (top) and perpendicular to the hexagonal channels (bottom).

The photopolymerization was carried out at 0 °C under N_2, using a light (400 nm) emitting diode. The medial (e.g., 9,10-) C−H out-of-plane (oop) bend at 897 cm^{-1} that is characteristic of anthracenes disappears upon photopolymerization and is replaced by the corresponding CH bend at 754 cm^{-1} that is characteristic of dianthracenes (Figure 3).[27] The disappearance of the 897-cm^{-1} band establishes the dimerization of the bridgehead anthracene groups with a degree of conversion above 90%. Residual benzene solvate appears as a peak at 695 cm^{-1}.

Spectroscopy also establishes the microstructure of the polymer. To test the hypothesis that antrip polymerizes by dimerization of its anthraceno blades at the medial positions, we labeled these positions with deuterium.[28] The IR spectra of labeled antrip, labeled polyantrip, and the analogous labeled anthracenes are shown in Figure 4. Upon irradiation, the original C−D stretch disappears and two new resonances appear. These new resonances correspond to the B_{1u} and B_{2u} combinations of C−D stretches in dianthracene.[27] Because the deuterium labels are introduced at specific positions, the differences in the IR spectra prove that crystalline antrip dimerizes at the medial positions.

This conclusion is reinforced by solid-state ^{13}C NMR studies.[29] The key observations are the appearance of a second bridgehead resonance in the $^1H-^{13}C$ correlation spectrum and a significant increased intensity of the bridgehead signal (Figure

dx.doi.org/10.1021/ja404351p | J. Am. Chem. Soc. 2013, 135, 14134−14141

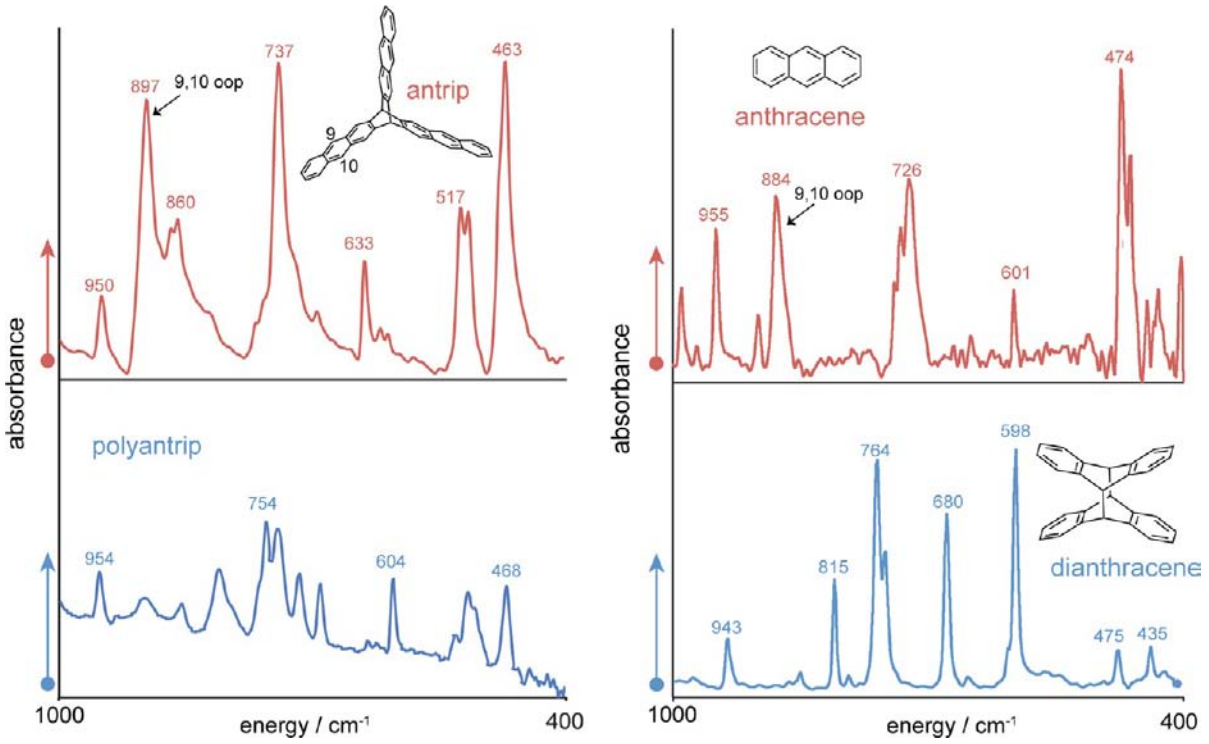

Figure 3. Left: IR spectrum of antrip (red) and polyantrip (blue). Note the disappearance of the 9,10 (medial) oop stretch at 897 cm^{-1}. Right: IR spectrum of anthracene (red) and dianthracene (blue).

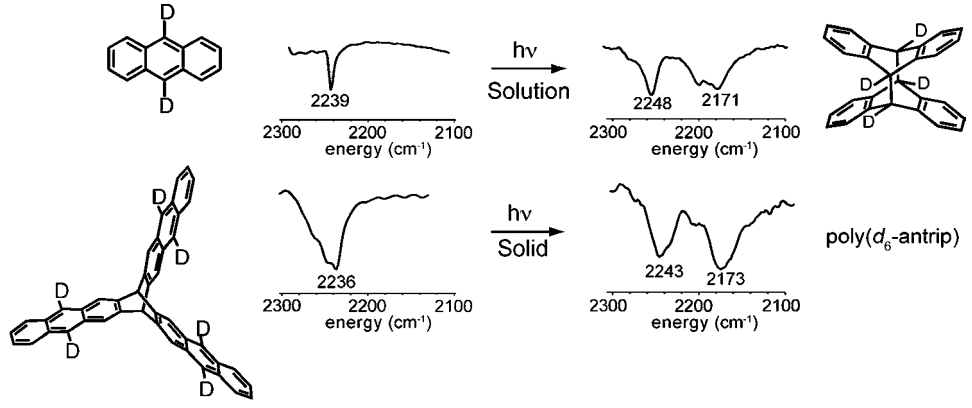

Figure 4. IR spectrum of deuterium-labeled antrip, polyantrip, and the model compounds demonstrating that polyantrip is cross-linked at the medial positions.

5). The ^{13}C chemical shifts of the triptycene-like bridgeheads and the dianthracene-like bridgeheads in polyantrip are expected to be close. The bridgehead ^{13}C chemical shifts of antrip (53.3 ppm), triptycene (54.1), and dianthracene (53.7) are all within 0.8 ppm, and their near degeneracy in the polyantrip ^{13}C spectrum is not surprising.

The identity of the repeat unit is established by depolymerization. Just as dianthracene thermolyzes to anthracene,[30] polyantrip thermolyzes to antrip. This thermolytic depolymerization, performed by microwave heating in d_6-DMSO at 200 °C, cleanly provides antrip (see the Supporting Information). The chemical yield, measured versus an internal standard by ^1H NMR, was 61%. Differential scanning calorimetry of polyantrip reveals the onset of the depolymerization exotherm at about 120 °C with a maximum at about 204 °C. The depolymerized residue recovered from the DSC pan was shown to be clean antrip by ^1H NMR spectrometry.

Powder X-ray diffraction before and after polymerization (Figure 6) establishes that the photopolymerization is a crystal-to-crystal transformation. Polyantrip shows sharp reflections and is therefore crystalline. The solid-state polymerization is not, however, a single-crystal to single-crystal transformation. The single crystals crack during irradiation, precluding single-crystal X-ray diffraction analysis. The similarity of the powder patterns of antrip and polyantrip reveals that the overall arrangement of fragments is similar in both structures. However, indexing of the powder pattern of polyantrip was highly ambiguous. All attempts at structural solution failed, including real-space methods using different unit cells from the indexing,[31] as well as model building followed by lattice-energy minimizations[32] and Rietveld refinements.[33]

Antrip polymerization was investigated by optical microscopy (OM) and scanning electron microscopy (SEM). The $P2_1/c$ polymorph of the benzene solvate forms parallelepipeds that

dx.doi.org/10.1021/ja404351p | J. Am. Chem. Soc. 2013, 135, 14134−14141

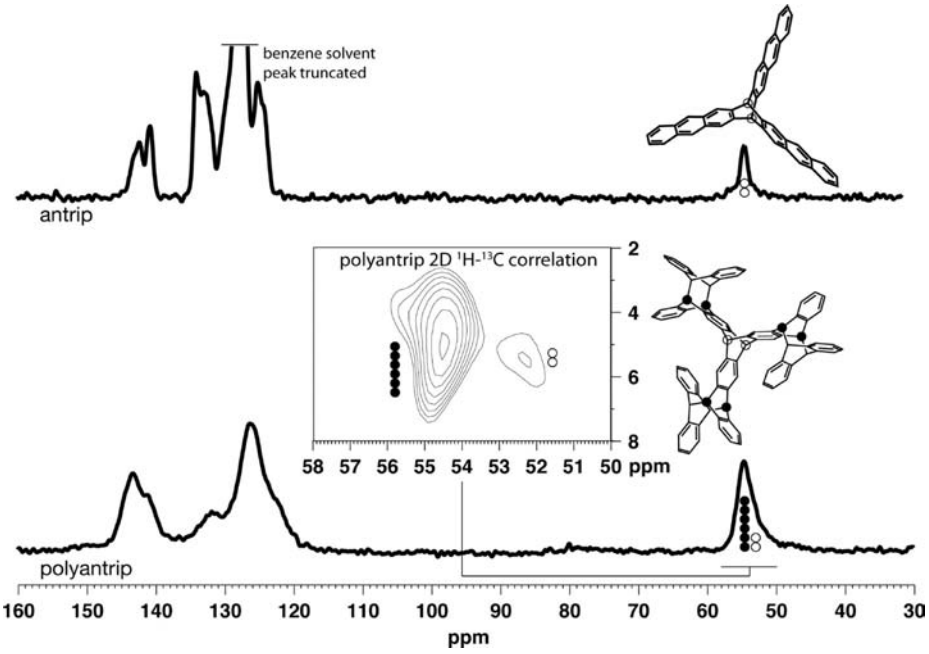

Figure 5. Solid-state NMR spectra[29] of antrip (benzene solvate) and polyantrip. Empty circles represent triptycene bridgehead carbons and filled circles represent dianthracene bridgehead carbons.

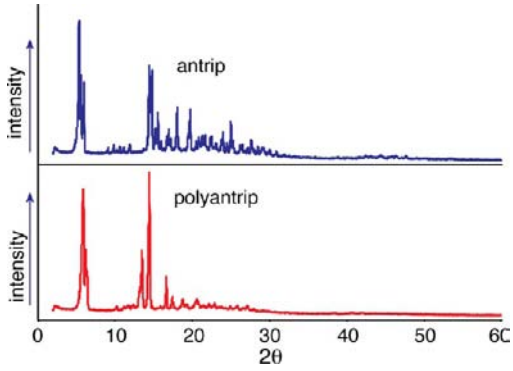

Figure 6. Powder X-ray diffraction pattern of antrip and polyantrip.

are strongly birefringent. Polyantrip retains the parallelepiped form and birefringence but cracks are evident in the scanning electron micrograph (Figure 7).

Polyantrip is insoluble in organic solvents, but the immersion of polyantrip blocks in selected solvents induces exfoliation. We surveyed 29 solvents (see the Supporting Information for details), selected according to Coleman's guidelines for graphene exfoliation,[14−16] for their ability to exfoliate polyantrip. The initial survey was monitored by optical microscopy. *N*-Methylpyrrolidone (NMP), quinoline, and cyclopentanone were identified as the most promising exfoliation solvents.

These three solvents were used for our exfoliation studies. Treatment with NMP at room temperature for 15 min caused the polyantrip blocks to separate into sheets that retained the form and dimensions of the crystal faces. Optical microscopy showed folds and overlaps. Quinoline at 25 °C only partially exfoliated polyantrip. A SEM image of quinoline-treated polyantrip revealed a side view of the sheets coming apart (Figure 7).

After several weeks in NMP, very thin sheets were obtained. These samples were deposited on a lacey carbon-coated TEM grid and observed by SEM. The NMP-exfoliated sheets were barely visible (Figure 8), but the layering or folding of thin sheets was evident after adjusting the image contrast. TEM imaging (see the Supporting Information for representative image) was less informative.

Atomic force microscopy (AFM) reveals individual steps in multilayered flakes (Figure 9). Height analysis suggests that these flakes are about 5 to 10 layers thick and steps corresponding to one or two layers are evident in the height analysis plots.

Extended exfoliation in NMP at ambient conditions affords single sheets of polyantrip. These single sheets are evident by AFM (Figure 10; a collection of single sheet images from

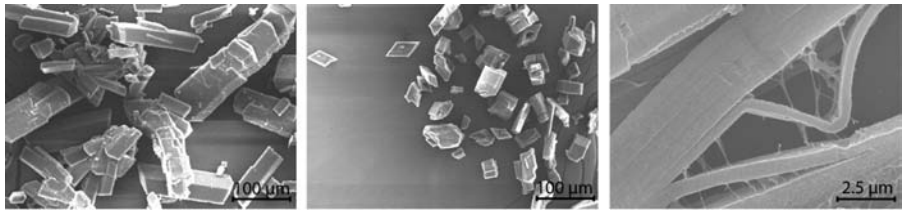

Figure 7. Scanning electron microscopy images: (left) antrip crystals; (middle) polyantrip; and (right) quinoline-treated polyantrip showing an edge-view of partial exfoliation.

dx.doi.org/10.1021/ja404351p | *J. Am. Chem. Soc.* 2013, 135, 14134−14141

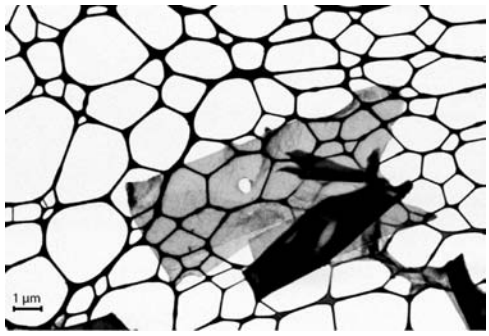

Figure 8. Contrast-enhanced negative SEM micrograph of polyantrip exfoliated by NMP.

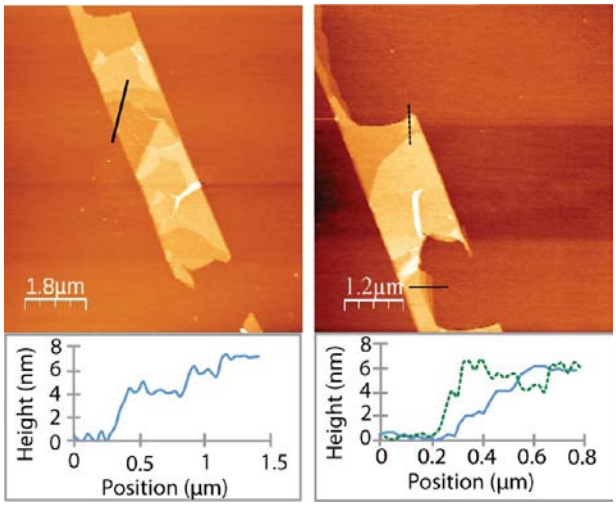

Figure 9. AFM images and height analysis of partially exfoliated polyantrip sheets on a mica substrate.

separate exfoliations can be found in the Supporting Information). The single sheets often appear to be lacy.

The lacy structure of the polyantrip sheets likely arises from depolymerization during exofoliation. To test the hypothesis that polyantrip partially depolymerizes during exfoliation, we looked by UV−vis spectrophotometry for the release of antrip during exfoliation at 50 and 80 °C in NMP. A few percent of free antrip was released in the first hours, followed by slow, linear release over a few weeks. This slow release of antrip is consistent with depolymerization. The depolymerization was about eight times faster at 80 °C than at 50 °C (Figure 11).

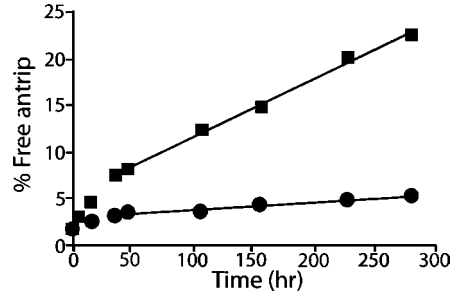

Figure 11. Depolymerization of polyantrip during exfoliation in NMP at 50 °C (circles) and 80 °C (squares). Reaction followed by UV absorbance at 361 nm.

■ DISCUSSION

The 2DP structures shown in Figure 12 are consistent with all observations. Depolymerization, IR spectroscopy, and solid-state NMR establish that the repeat unit is triple [4 + 4] adduct of the antrip monomer. IR spectrophotometry establishes that the extent of reaction is greater than 90%. SEM and AFM establish that the polyantrip exists as flat sheets. Powder diffraction shows that the material is periodic and that the spatial arrangement of fragments in the polymer is similar as in the antrip monomer.

The theory of tilings allows us to propose a structure for polyantrip based on the findings described in the previous paragraph. As stated in the introductory paragraph, we consider the polyantrip 2DP as a tiling with RUs corresponding to vertices and the linkages between the RUs corresponding to edges. We define the valence of the vertex to be the number of linkages that the RU forms. The vertices and edges form tiles, and these tiles cover the plane.

If we assume that the antrip RU has a valence of three, which is established by the monomer structure, and that the structure is periodic, which is established by powder X-ray diffraction, then it can be mathematically proven that the average number

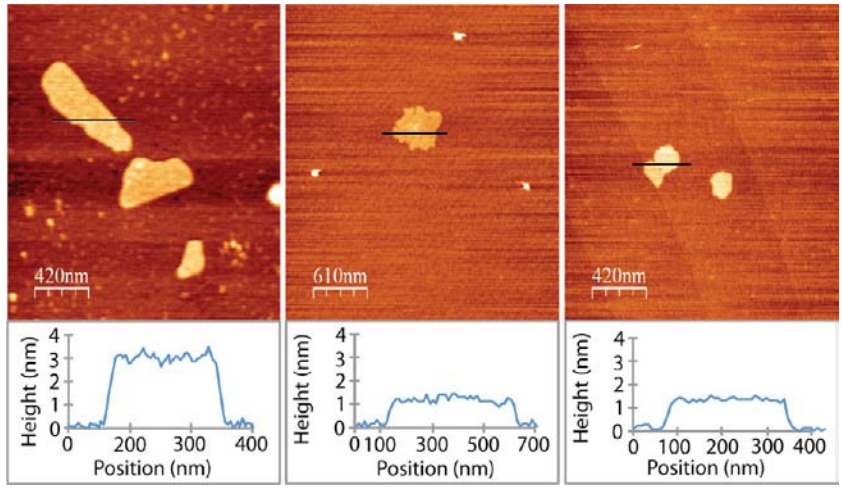

Figure 10. AFM images and height analysis of few- and single-layer polyantrip sheets on a mica substrate.

dx.doi.org/10.1021/ja404351p | J. Am. Chem. Soc. 2013, 135, 14134−14141

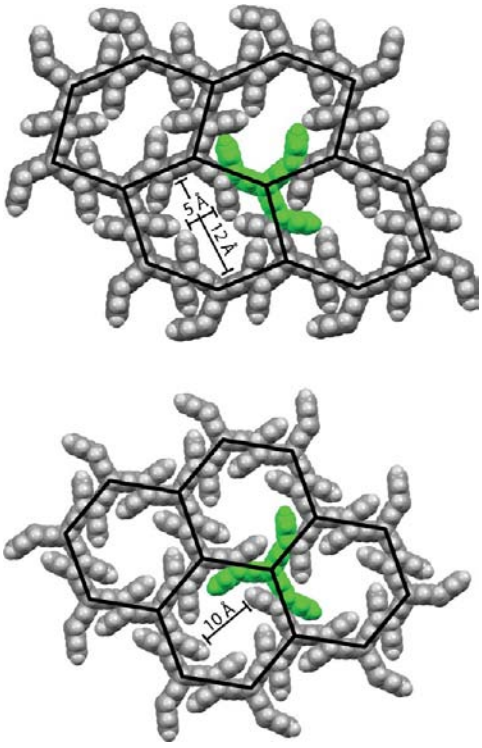

Figure 12. Two possible structures for polyantrip.

of edges of the tiles is six.[34] Both the honeycomb tiling and the pentaheptite lattice[35] shown in Figure 13 have an average of six

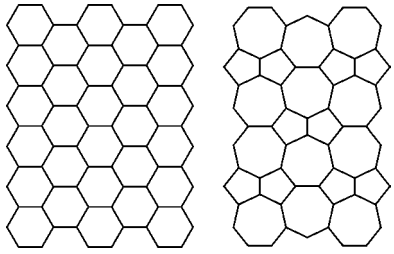

Figure 13. Two mathematically permissible graphs that represent polyantrip's connectivity: (left) the honeycomb lattice and (right) a pentaheptite lattice. Note that these diagrams are connectivity graphs and do not represent atoms and bonds in the normal sense.

edges per tile and satisfy this requirement. The 3.12^2 and 4.6.12 Archimedean lattices[34] also satisfy this condition but would give packings with unreasonably low densities and can therefore be disregarded.

Antrip's 120° angle matches the hexagons of the honeycomb lattice. Any other lattice requires pentagons and heptagons, or squares and octagons, etc. While we cannot rigorously exclude other lattices, e.g. a pentaheptite lattice, the 120° angles of the triptycene core naturally fit the honeycomb lattice and we strongly suspect that the lattice is a honeycomb structure. The structure must be a honeycomb if only one type of tile is present because, as shown above, the average tile has six sides. We have not, however, established that only one type of tile is present.

Let us reasonably assume a honeycomb lattice. This honeycomb lattice only conveys the connectivity of the 2DP, and, of course, stereochemistry must be considered. Each anthraceno blade of the antrip RUs will kink upon photodimerization. These kinks can form in the same sense, giving rise to a C_{3h} RU, or two kinks can form in the same sense and one kink can form in the opposite sense, giving rise to a C_s RU. These motifs are highlighted in green in Figure 12. In a honeycomb lattice, the C_{3h} RUs give the plane group *p6* and the C_s RUs give the plane group *p2gg*. More complex tilings having both the C_{3h} and C_s RUs can be envisioned.

The proposed structures for these 2DPs (Figure 12) are porous. In the *p2gg* packing, the cross section of the solvent accessible[36] pores is 85 Å^2, and the pores cover 28% of the area. In the *p6* packing, the cross section of the solvent accessible pores is 98 Å^2, and the pores cover 32% of the area. If we consider the pores to be simple circles, their diameter will be ~10 Å. Both structures will have $\sim 3.3 \times 10^{12}$ pores/cm^2.

The formation of polyantrip sheets by the photopolymerization of monomer crystals that lack lamellar structure is not particularly surprising. The topochemical hypothesis only states that, "reaction in the solid state occurs with a minimum amount of atomic or molecular movement";[37] movement is allowed, and the required planarization requires only the tilt of antrip molecules. All anthracene blades are within the 4.2 Å distance that is normally expected for a topochemical reaction. Indeed, large movements are observed in solid-state reactions and are sufficiently common to earn designations such as "topochemically forbidden"[23] or "anomalous"[38] solid-state reactions. The solid-state photodimerization of 9-cyano anthracene,[39] which packs in a head-to-head arrangement but gives only head-to-tail photodimers, has been known for more than forty years and has been widely studied.[23,40] A recent photophysical study[41] on the anomalous solid-state photodimerization of 9-anthracenecarboxylic acid adds "more puzzle parts" to the mechanism of these complex solid-state photoreactions. The mechanism of these reorganizations is not fully understood but is thought to involve rearrangements through voids or defects.[38,42] Kaupp stridently argues[43,44] against the dominance of the topochemical hypothesis[23] in the analysis of solid-state reactions. In their 2004 review[45] on solid-state reactions, Braga and Grepioni state that, "Many solid-state reactions give a near quantitative yield of a single product and require high molecular mobility." The movement of antrip monomers during solid-state photodimerization is not surprising, although the exact mechanism of the transformation remains unclear.

An analysis of the thermodynamics of the anthracene dimer allows us to understand the depolymerization of polyantrip that can occur during exfoliation. The dissociation of dianthracene to two molecules of anthracene is exothermic (ΔH, $\sim -1 \times 10^1$ kcal/mol).[46] Polyantrip exothermically depolymerizes (established by differential scanning calorimetry) to antrip (established by ^{1}H NMR) starting at about 120 °C. And because ΔS of depolymerization is surely positive, the depolymerization of polyantrip to antrip is spontaneous ($\Delta G < 0$) at all temperatures. Linear polymers containing main-chain dianthracene linkages are also thermally sensitive, often breaking down above 90 °C.[47]

The lacy structure occasionally observed by AFM of aggressively exfoliated samples suggests that depolymerization occurs from the edges and proceeds inward. Similar lacy patterns were recently observed in the etching of graphene.[48] The lacy patterns suggest that the partially linked, peripheral antrip RUs are more labile than the fully linked, internal antrip RUs. This depolymerization from the edges inward is the two-dimensional analogue of the unzipping of 1-D polymers, e.g.

dx.doi.org/10.1021/ja404351p | J. Am. Chem. Soc. 2013, 135, 14134−14141

the depolymerization of poly(oxymethylene) that occurs from the ends.

CONCLUSION

We have prepared a 2DP by the solid-state photopolymerization of crystalline antrip. The polyantrip 2DP can be exfoliated to single sheets. Some depolymerization is observed at moderate (50 °C) temperatures. Vibrational spectra, especially the deuterium labeling studies, and solid-state NMR measurements establish the microstructure of polyantrip. Depolymerization establishes the identity of the repeat unit. Microscopy established the presence of large, flat faces. These observations, taken together and analyzed in the context of tiling theory, are consistent with the structures shown in Figure 12.

ASSOCIATED CONTENT

Supporting Information

Detailed synthetic procedure and spectra for all compounds, crystallographic information files for various antrip polymorphs and solvates, and original, full resolution images. This material is available free of charge via the Internet at http://pubs.acs.org.

AUTHOR INFORMATION

Corresponding Author

king@chem.unr.edu

Notes

Notes. The authors declare no competing financial interest.

ACKNOWLEDGMENTS

We thank the US-NSF (CHE-0957702 and CHE-0947088) for support, Dr. René Verel for acquisition of the solid-state NMR spectra, Mr. Carey Johnson and Dr. Patrick Kissel for assistance with modeling, Edith Alig (Frankfurt University) for the acquisition of X-ray powder data, and Stefan Habermehl (Frankfurt University) for assistance on attempts to solve the crystal structure of polyantrip from powder data.

REFERENCES

(1) O'Keeffe, M.; Hyde, B. G. *Philos. Trans. R. Soc., A* **1980**, *295*, 553−618.
(2) Sakamoto, J.; van Heijst, J.; Lukin, O.; Schlüter, A. D. *Angew. Chem., Int. Ed.* **2009**, *48*, 1030−1069. Coulson, J. W.; Dichtel, W. R. *Nat. Chem.* **2013**, *5*, 453−465.
(3) Novoselov, K. S. *Rev. Mod. Phys.* **2011**, *83*, 837.
(4) Kissel, P.; Erni, R.; Schweizer, W. B.; Rossell, M. D.; King, B. T.; Bauer, T.; Götzinger, S.; Schlüter, A. D.; Sakamoto, J. *Nat. Chem.* **2012**, *4*, 287−291.
(5) Tahara, K.; Inukai, K.; Hara, N.; Johnson, C. A., II; Haley, M. M.; Tobe, Y. *Chem.−Eur. J.* **2010**, *16*, 8319−8328.
(6) Bieri, M.; Nguyen, M.-T.; Gröning, O.; Cai, J.; Treier, M.; Aït-Mansour, K.; Ruffieux, P.; Pignedoli, C. A.; Passerone, D.; Kastler, M.; Müllen, K.; Fasel, R. *J. Am. Chem. Soc.* **2010**, *132*, 16669−16676.
(7) Abel, M.; Clair, S.; Ourdjini, O.; Mossoyan, M.; Porte, L. *J. Am. Chem. Soc.* **2011**, *133*, 1203−1205.
(8) Colson, J. W.; Woll, A. R.; Mukherjee, A.; Levendorf, M. P.; Spitler, E. L.; Shields, V. B.; Spencer, M. G.; Park, J.; Dichtel, W. R. *Science* **2011**, *332*, 228−231.
(9) Gee, G.; Rideal, E. K. *Proc. R. Soc. London, Ser. A* **1935**, *153*, 116−128.
(10) Kunitake, T. *Macromol. Symp.* **1995**, *98*, 45−51.
(11) Michl, J.; Magnera, T. F. *Proc. Natl. Acad. Sci. U.S.A.* **2002**, *99*, 4788−4792.
(12) Bauer, T.; Schlüter, A. D.; Sakamoto, J. *Synlett* **2010**, *6*, 877−880.
(13) Bauer, T.; Zheng, Z.; Renn, A.; Enning, R.; Stemmer, A.; Sakamoto, J.; Schlüter, A. D. *Angew. Chem., Int. Ed.* **2011**, *50*, 7879−7884.
(14) Khan, U.; O'Neill, A.; Lotya, M.; De, S.; Coleman, J. N. *Small* **2010**, *6*, 864−871.
(15) O'Neill, A.; Khan, U.; Nirmalraj, P. N.; Boland, J.; Coleman, J. N. *J. Phys. Chem. C* **2011**, *115*, 5422−5428.
(16) Coleman, J. N.; Lotya, M.; O'Neill, A.; Bergin, S. D.; King, P. J.; Khan, U.; Young, K.; Gaucher, A.; De, S.; Smith, R. J.; Shvets, I .V.; Arora, S. K.; Stanton, G.; Kim, H.-Y.; Lee, K.; Kim, G. T.; Duesberg, G. S.; Hallam, T.; Boland, J. J.; Wang, J. J.; Donegan, J. F.; Grunlan, J. C.; Moriarty, G.; Shmeliov, A.; Nicholls, R. J.; Perkins, J. M.; Grieveson, E. M.; Theuwissen, K.; McComb, D. W.; Nellist, P. D.; Nicolosi, V. *Science* **2011**, *331*, 568−571.
(17) Ma, R.; Sasaki, T. *Adv. Mater.* **2010**, *22*, 5082−5104.
(18) Berlanga, I.; Ruiz-González, M. L.; González-Calbet, J. M.; Fierro, J. L. G.; Mas-Ballesté, R.; Zamora, F. *Small* **2011**, *7*, 1207−1211.
(19) Spitler, E. L.; Koo, B. T.; Novotney, J. L.; Colson, J. W.; Uribe-Romo, F. J.; Gutierrez, G. D.; Clancy, P.; Dichtel, W. R. *J. Am. Chem. Soc.* **2011**, *133*, 19416−19421.
(20) Amo-Ochoa, P.; Welte, L.; González-Prieto, R.; Sanz Miguel, P. J.; Gómez-García, C. J.; Mateo-Martí, E.; Delgado, S.; Gómez-Herrero, J.; Zamora, F. *Chem. Commun.* **2010**, *46*, 3262.
(21) Gallego, A.; Hermosa, C.; Castillo, O.; Berlanga, I.; Gómez-García, C. J.; Mateo-Martí, E.; Martínez, J. I.; Flores, F.; Gómez-Navarro, C.; Gómez-Herrero, J.; Delgado, S.; Zamora, F. *Adv. Mater.* **2013**, *25*, 2141−2146.
(22) Wegner, G. Z. *Naturforscher* **1969**, *24B*, 824−832.
(23) Schmidt, G. M. *Pure Appl. Chem.* **1971**, *27*, 647−678.
(24) Long, T. M.; Swager, T. M. *Adv. Mater.* **2001**, *13*, 601−604.
(25) Luo, J.; Hart, H. *J. Org. Chem.* **1987**, *52*, 3631−3636.
(26) Additional crystallographic details are included in the Supporting Information.
(27) For 9,10 oop modes in anthracene, see: Singh, S.; Sandorfy, C. *Can. J. Chem.* **1969**, *47*, 257−263. The corresponding vibrational modes in dianthracene were identified by comparing the IR spectrum of bridgehead-deuterated dianthracene with the IR spectrum of unlabeled dianthracene.
(28) Kachkurova, I. Y. *J. Appl. Spectrosc.* **1975**, *22*, 522−526.
(29) The spectra were measured on a 700 MHz (^{1}H nominal frequency, 16.4 T) magnet with a nominal ^{13}C frequency of 175 MHz using cross-polarization methods. A 2.5 mm rotor that was filled to capacity was spun at 24 kHz.
(30) Breton, G. W.; Vang, X. *J. Chem. Educ.* **1998**, *75* (1), 81−82.
(31) David, W. I. F.; Shankland, K.; van de Streek, J.; Pidcock, E.; Motherwell, W. D. S.; Cole, J. C. *J. Appl. Crystallogr.* **2006**, *39*, 910−915.
(32) Accelrys Inc., *Materials Studio 4.4*; Accelrys Inc.: San Diego, CA, USA, 2008.
(33) Coelho, A.A.; *TOPAS Academic 4.1*, 2007.
(34) The connection between the average number of edges and the valence of the vertices is a consequence of Euler's Theorem for Tilings. A proof of this connection can be found in the following: Grünbaum, B.; Shephard, G. C. *Tilings and Patterns*; W. H. Freeman and Company: New York, NY, 1987; pp 139−141.
(35) Deza, M.; Fowler, P. W.; Shtogrin, M.; Vietze, K. *J. Chem. Inf. Comput. Sci.* **2000**, *40*, 1325−1332.
(36) The pore diameter was determined by cutting and weighing a paper printout of the proposed polymer structures as viewed down the channels. The channels were defined by using the void feature of Mercury with a 1.2 Å probe to determine the contact surface. Macrae, C. F.; Bruno, I. J.; Chisholm, J. A.; Edgington, P. R.; McCabe, P.; Pidcock, E.; Rodriguez-Monge, L.; Taylor, R.; van de Streek, J.; Wood, P. A. *J. Appl. Crystallogr.* **2008**, *41*, 466−470.
(37) Cohen, M. D.; Schmidt, G. M. J. *J. Chem. Soc.* **1964**, 1996−2000.
(38) Thomas, J. M. *Pure Appl. Chem.* **1979**, *51*, 1065−1082.
(39) Craig, D. P.; Sarti-Fantoni, P. *Chem. Commun. (London)* **1966**, 742−743.

(40) Cohen, M. D.; Ludmer, Z.; Thomas, J. M.; Williams, J. O. *J. Chem. Soc. D* **1969**, 1172−1173.
(41) Moré, R.; Busse, G.; Hallmann, J.; Paulmann, C.; Scholz, M.; Techert, S. *J. Phys. Chem. C* **2010**, *114*, 4142−4148.
(42) Enkelmann, V. *Adv. Polym. Sci.* **1984**, *63*, 91−136.
(43) Kaupp, G. *CrystEngComm* **2003**, *5*, 117−133.
(44) Kaupp, G. *Curr. Opin. Solid State Mater. Sci.* **2002**, *6*, 131−138.
(45) Braga, D.; Grepioni, F. *Angew. Chem. Int. Ed.* **2004**, *43*, 4002−4011.
(46) Grimme, S.; Diedrich, C.; Korth, M. *Angew. Chem., Int. Ed.* **2006**, *45*, 625−629.
(47) Tazuke, S.; Tanabe, T. *Macromolecules* **1979**, *12*, 848−853.
(48) Geng, D.; Wu, B.; Guo, Y.; Luo, B.; Xue, Y.; Chen, J.; Yu, G.; Liu, Y. *J. Am. Chem. Soc.* **2013**, *135*, 6431−6434.